SANDIA REPORT

SAND2016-12948
Unlimited Release
Printed December 2016

Uncertainty Quantification of Pressurization Due to Organic Material Decomposition

Ryan Keedy

Prepared by
Sandia National Laboratories
Albuquerque, New Mexico 87185 and Livermore, California 94550

Sandia National Laboratories is a multi-mission laboratory managed and operated by Sandia Corporation, a wholly owned subsidiary of Lockheed Martin Corporation, for the U.S. Department of Energy's National Nuclear Security Administration under contract DE-AC04-94AL85000.

Issued by Sandia National Laboratories, operated for the United States Department of Energy by Sandia Corporation.

Available to DOE and DOE contractors from
U.S. Department of Energy
Office of Scientific and Technical Information
P.O. Box 62
Oak Ridge, TN 37831

Telephone: (865) 576-8401
Facsimile: (865) 576-5728
E-Mail: reports@osti.gov
Online ordering: http://www.osti.gov/scitech

Available to the public from
U.S. Department of Commerce
National Technical Information Service
5301 Shawnee Rd
Alexandria, VA 22312

Telephone: (800) 553-6847
Facsimile: (703) 605-6900
E-Mail: orders@ntis.gov
Online order: http://www.ntis.gov/search

SAND2016-12948
Unlimited Release
Printed December 2016

Uncertainty Quantification of Pressurization due to Organic Material Decomposition

Ryan Keedy
Thermal/Fluid Science and Engineering
Sandia National Laboratories
P.O. Box 969
Livermore, CA 94550-MS9957

Abstract

A new approach for describing the uncertainty associated with organic material decomposition in an abnormal thermal environment is described. Rather than applying multipliers to the pressure predicted by the simulation, the uncertain parameters are incorporated in a broader Latin hypercube sampling study. The resulting distribution gives more information than the pressure multiplier, but similar uncertainty bounds can be derived from a log-normal fit.

ACKNOWLEDGMENTS

I would like to thank Adam Hetzler, Cosmin Safta, and Patty Hough for reviewing this manuscript and providing valuable feedback as it pertains to uncertainty quantification. Their input not only helped make this report better, but it also provided significant food for thought when it comes to future work.

I would also like to especially thank Sarah Scott and Victor Brunini for the time and attention they gave to help review and refine this manuscript as part of their ongoing support of the improvement of organic material modeling in abnormal thermal environments.

CONTENTS

1. Introduction 8
1.1. Background 8
1.2. Description of Experiment 11
1.3. Description of Simulation 12
2. Latin Hypercube Sampling Study 14
2.1. Description of LHS Study 14
2.2. Pressure Distribution 15
2.3. Effect of Number of Runs 17
2.4. Time Dependency 19
2.5. Parameter Sensitivity 21
2.6. Comparison to Experiment 23
3. Discussion 25
4. References 26
Distribution 27

FIGURES

Figure 1: Pressure uncertainty multiplier break-out 10
Figure 2: FIC experiment: (a) experimental setup of the foam-in-can experiments, (b) description of upright and inverted orientations, and (c) an exploded view of the geometry 11
Figure 3: Diagram of foam-in-can geometry with thermocouple locations illustrated 11
Figure 4: Pressure-time histories of foam-in-can experiments in both upright and inverted configurations (50 °C/min, 20 lb/ft^3 PMDI foam) 12
Figure 5: Finite element mesh of the foam-in-can geometry; cutaway to illustrate the interior element size 13
Figure 6: Histogram of final pressure from 640 LHS simulations 16
Figure 7: Histogram of final pressure from 640 LHS simulations, with log-normal distribution fit to the data 17
Figure 8: Fitted log-normal distributions for LHS studies of various sizes (80-640 simulations) 18
Figure 9: Upper and lower bounds, as well as the mode of the fitted log-normal distribution as a function of the size of the LHS study 18
Figure 10: Comparison of UQ bounds defined by the pressure multiplier (green) the time-dependent log-normal distribution (cyan), and the min/max from the LHS simulations (magenta) 19
Figure 11: Zoomed in view of data from Figure 10 from 0 to 500 seconds 20
Figure 12: Early time (100 sec) distribution of pressures produced by the LHS study 21
Figure 13: Example of a time (450 sec) when a LHS simulation predicts a pressure outside of the bounds of the log-normal distribution 21
Figure 14: Pearson correlation coefficients of all nine parameters with respect to pressure as a function of time 22
Figure 15: Comparison of upright and inverted experiments to simulation with calculated uncertainty 23

TABLES

Table 1: Uncertain parameter multipliers assigned normal distributions 14
Table 2: Uncertain parameter multipliers assigned uniform distributions 15
Table 3: Uncertain parameter multipliers assigned triangular distributions 15

NOMENCLATURE

FIC	foam-in-can
LHS	Latin hypercube sampling
UQ	uncertainty quantification
REF	removable epoxy foam
PMDI	polymeric methylene diisocyanate
TGA	thermo-gravimetric analysis
CDF	cumulative distribution function
PDF	probability distribution function
OMD	organic material decomposition

1. INTRODUCTION

The goal of the present work is to describe a new approach for quantifying the pressure uncertainty for foam decomposing in a volume. The thermal analyses were conducted using the multi-physics code Aria, part of the Sierra simulation suite [1]. The previous approach for bounding the pressurization uncertainty is explained, and justification for the new model is given. Results produced by the new uncertainty quantification procedure are analyzed, and differences between the approaches are explained.

1.1. Background

Uncertainty quantification (UQ) analyses of thermal simulations are often conducted by running an ensemble of Latin hypercube sampling (LHS) simulations (e.g. [2], [3], [4], [5]). The simulation parameters are varied randomly, but systematically, to comprehensively explore the parameter space efficiently. The results also provide a basis for evaluating the sensitivities of responses of interest to each parameter. See [6] and [7] for a more thorough description of the LHS method. Implementation of the LHS approach and processing of the responses is performed using Dakota [8] and a series of python scripts.

The previous approach to estimate uncertainty of the pressurization deviated from the method of assessing the uncertainty associated with other simulation parameters. Typically, when evaluating simulation outputs (e.g. temperature), the range of responses given the uncertainty of the parameter inputs is of interest. Oftentimes, this range is presented as a multiple of the standard deviation of the results (assuming a normal distribution). However, the uncertainty of the pressure of a foamed region has typically been presented as a multiple of the pressure predicted by the nominal simulation (using all nominal parameter values), e.g.

$$\boldsymbol{P}_{UQ} = \boldsymbol{\lambda P}$$

where P_{UQ} is the pressure associated with the uncertainty of the simulation (esp. regarding model form error), λ is an uncertainty multiplier, and p is the pressure associated with the Aria output of the nominal simulation. From [9], referring to REF foam (bold added for emphasis):

> The pressure uncertainty multiplier, λ, spans the range of 0.5 to 2.2. This variation is based on the following physical arguments. In the chemistry model, pressure increase is a result of gas product production due to pyrolysis reactions that occur because of an increase in temperature within a constrained volume. The volume available to the gas is uncertain because the foam is initially closed cell and the pore structure opens as pressure and temperature increase. In addition, the formation of liquid and potentially a liquid layer influences the volume available to the gas. When REF decomposes, it produces smaller polymer fragments that can be distributed between the gaseous and liquid phases depending upon pressure and temperature and a vapor-liquid equilibrium balance. In this model, thermal equilibrium between phases is assumed, and the heat transfer through the foam has errors associated with it, therefore the temperature at which reactions occur is uncertain, thus causing the moles of gas calculated to be uncertain. Model form

errors were assigned with minimum and maximum multipliers: the amount of material in the gas phase has a multiplier of 0.7 to 1, the temperature of the gas associated with the number of moles of gas produced has a multiplier of 0.8 to 1.2, the volume that the gas occupies has a multiplier of 0.6 to 1.0, and the temperature of the entire gas phase has a multiplier of 0.9 to 1.1. Combining the minimum and maximum values in the ideal gas equation and calculating the pressure results in **estimated bounds of uncertainty from 50% to 220% of the nominal prediction**. Since this error dominates the other sources of uncertainty, the results of the pressure prediction will be presented both with and without this error included.

The nominal Aria simulation represents the case where each of the four multipliers has a value of unity. The physical interpretation is that in the simulation, all of the decomposed foam mass is converted to the gas phase, and the maximum volume is available for gas to expand into (i.e. all the foam porosity is available for gas products). The Aria simulation is agnostic with regards to the temperature of the entire gas phase and the temperature of the gas phase associated with the number of moles of gas produced.

With this approach, the pressure is calculated with the ideal gas law via a plugin. Four parameters are incorporated into the uncertainty multiplier:

1. Number of moles of decomposition products in gas phase
2. Total number of moles of decomposition products
3. Volume available for gas
4. Bulk gas phase temperature

See Figure 1 for a break-out of the uncertainty contributions to the ideal gas calculation. The approach of this study is to reincorporate the uncertain parameters influencing pressurization back into the LHS study and evaluate them in a manner consistent with the rest of the uncertain model parameters.

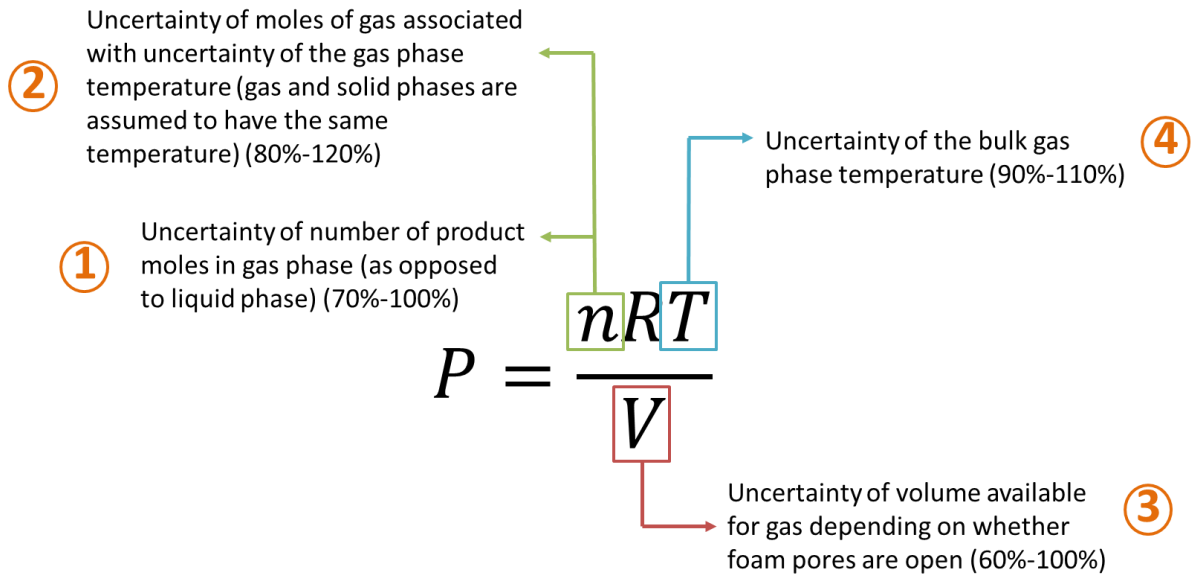

Figure 1: Pressure uncertainty multiplier break-out

The uncertain parameters described in Figure 1 can be represented by applying uncertainty bounds to simulation inputs. For instance, the uncertainty of the number of moles of product in the gas phase (as opposed to the liquid phase) is treated by varying the proportion of decomposition products that are treated as char versus gas. In the nominal simulation parameters, it is assumed that there is no liquid phase; all decomposition products exist in either the gas phase as CO_2 or higher molecular weight organics, or in the solid phase as char. However, under pressure, it is expected that some gases may condense.

An additional uncertain parameter that has a direct impact on the number of moles in the gas phase is the molecular weight of the products themselves. For example, if a fixed mass of foam decomposes into products with a modeled molecular weight of X as opposed to Y, the resulting number of moles will be a multiple of Y/X.

The uncertainty about the volume available for gas is addressed by adjusting the initial porosity of the foam. Under the current model implementation, any porous volume in the region is assumed to allow for gas expansion. However, many of the virgin foams under consideration (e.g. PMDI) are known to be closed cell, i.e. have zero permeability. Therefore, at low pressure and temperature, it is not expected to be an available volume into which product gases can flow. As a work-around, the solid density of the foam can be redefined to artificially lower the porosity to reflect the closed-pore state for the purpose of pressurization calculations.

The pressure uncertainty due to temperature uncertainties described in Figure 1, especially points #2 and #4, are not explicitly accounted for in this analysis. Instead, additional parameters' uncertainties (e.g. foam conductivity) will influence the temperature indirectly, which will in turn influence decomposition progression and pressure.

1.2. Description of Experiment

The simulations are set up to mimic six foam-in-can (FIC) experiments from 2013 [10]. The heating rate of the experiments in question was 50 ºC/min. The polymeric methylene diisocyanate (PMDI) foam decomposition model used in this paper has been validated against these experiments in [5]; additional simulations have been performed and compared to similar FIC experiments in [2] and [11].

In short, each FIC test consisted of a stainless steel can measuring approximately 3.5" in diameter and 3" high. The can had a hollowed out space at one end that is partially filled with an embedded metal object (stainless steel). The interior of the can is filled with a piece of PMDI foam machined to be a press-fit into the container before welding the stainless steel container shut.

Figure 2 illustrates several aspects of the experimental setup.

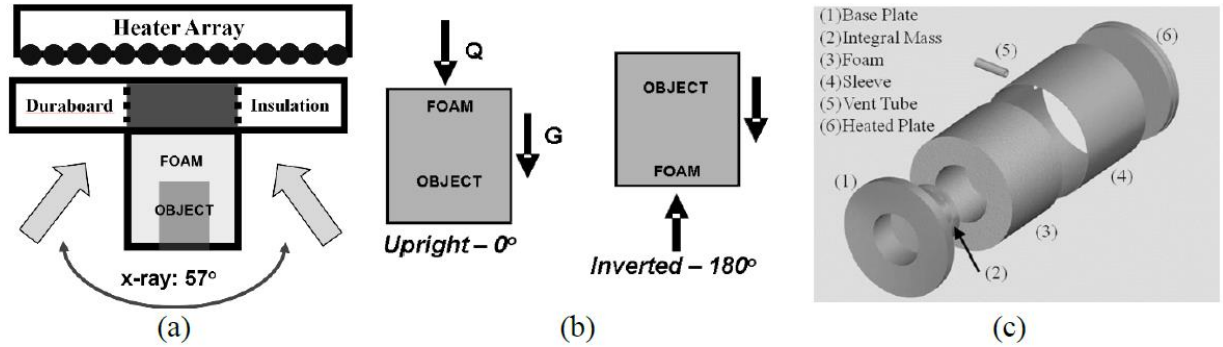

Figure 2: FIC experiment: (a) experimental setup of the foam-in-can experiments, (b) description of upright and inverted orientations, and (c) an exploded view of the geometry

In addition to a pressure tap monitoring the pressure inside the can during the experiment, there were a number of thermocouples throughout the can to measure temperatures as a function of time during the experiment (see Figure 3).

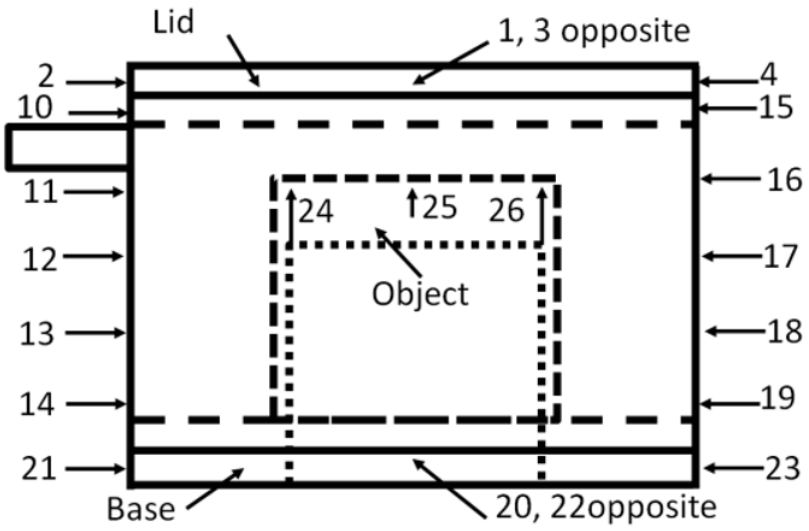

Figure 3: Diagram of foam-in-can geometry with thermocouple locations illustrated

The experiments were performed three times in the upright configuration and three times in the inverted configuration (see Figure 2(b)). The orientation of the can with respect to gravity has been observed to impact the pressure-time history of the test. Figure 4 illustrates the differences in pressure response between upright and inverted cases. The inverted case pressurizes appreciably faster than the upright case. It is believed that this is due to a gravity-driven differentiation of gas and liquid movement throughout the can.

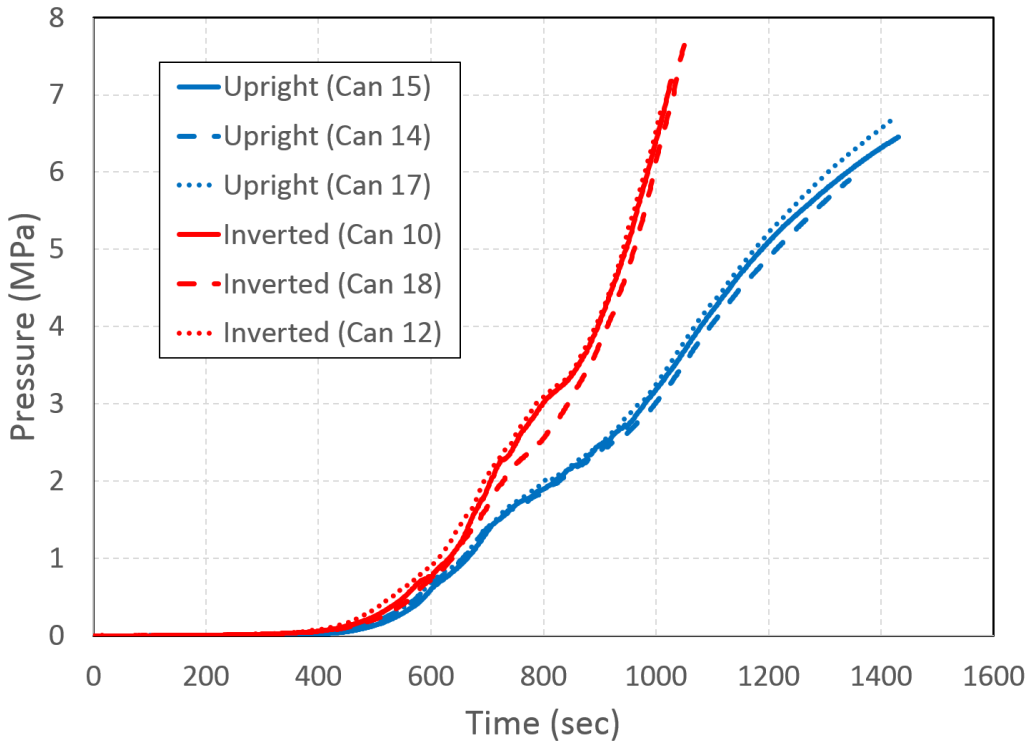

Figure 4: Pressure-time histories of foam-in-can experiments in both upright and inverted configurations (50 °C/min, 20 lb/ft^3 PMDI foam)

1.3. Description of Simulation

The simulations were conducted with Aria, a multi-physics solver package that is part of the Sierra simulation suite [1]. The simulations were conducted using a finite element mesh containing 57,732 elements and 13,848 nodes (26,311 elements, 5,417 nodes in the foam block; 31,421 elements, 8,431 nodes in the container block) – see Figure 5.

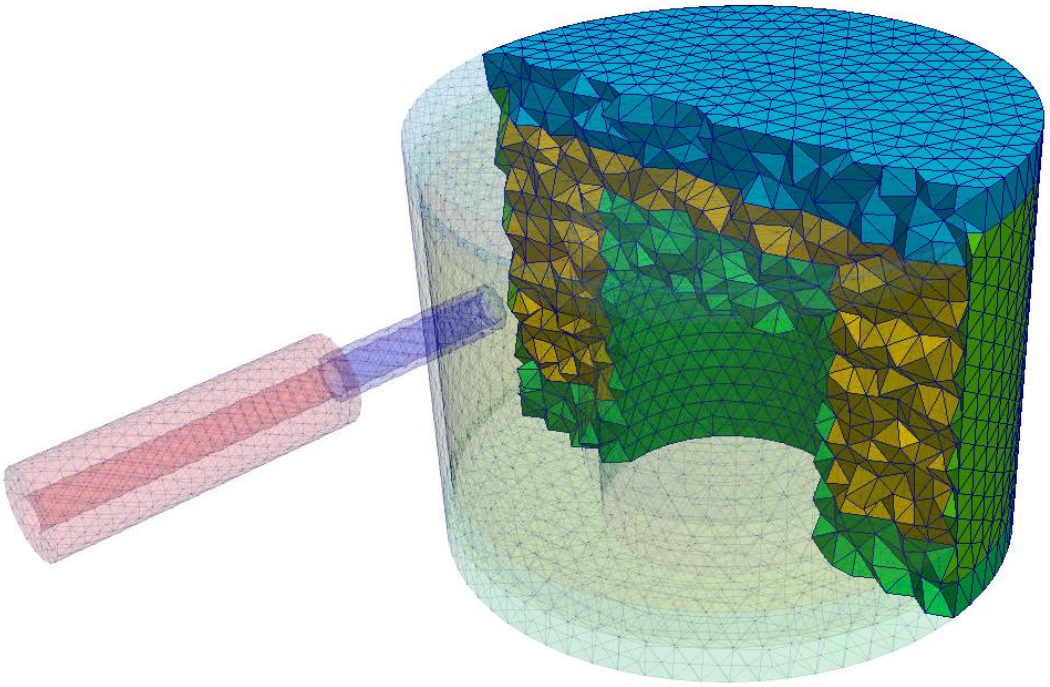

Figure 5: Finite element mesh of the foam-in-can geometry; cutaway to illustrate the interior element size

The models are well described in [5], including a description of the chemical processes involved in the decomposition of PMDI. The description and implementation of the thermal conductivity of the PMDI foam has been changed slightly, which is described in [12].

2. LATIN HYPERCUBE SAMPLING STUDY

2.1. Description of LHS Study

The LHS study included nine parameters which were varied according to expert opinion as well as historical precedent. The parameters can be divided in two main categories, covering the physics before and during thermal decomposition:

Virgin Foam Properties:

- Thermal conductivity of foam
- Specific heat of foam
- Bulk density of foam
- Porous volume available to the gas

Decomposition Parameters:

- Activation energy of foam decomposition
- Heat of reaction of foam decomposition
- Fraction of "gaseous" products in the gas phase
- Char mass fraction of decomposition products
- Molecular weight of "gaseous" products

There are a number of ways to define the distribution of the uncertainty of the various model parameters. The three distributions considered in this document are normal (Gaussian), triangular, and uniform. The distribution parameters detailed below are non-dimensionalized and applied as multipliers to the relevant model parameters.

The Gaussian distribution is the default assumption for unknown quantities, however, care must be taken when applying this type of distribution. If it is applied to a physically bounded quantity (e.g. emissivity, $0 \leq \varepsilon \leq 1$), there is a possibility that large deviations would lead to samples outside of the physical bounds. Table 1 details the two parameters that are modeled with normal distributions. Because the heat of reaction has a mean of zero, the standard deviation cannot be given as a percentage of the mean; instead, it is given in units of J/kg (applies to all three reactions).

Table 1: Uncertain parameter multipliers assigned normal distributions

Parameter	Mean	Std. Dev. (%)	Description
UQ_Ea	1.0	2	Activation energy of foam decomposition
UQ_HR	0.0	1e5*	Heat of reaction of foam decomposition

Some model parameters can be bracketed fairly reliably (e.g. physical constraints, measurement data), but the exact value of the quantity is uncertain. In this case, a uniform distribution is assumed. See Table 2 for details of the five parameters that are varied uniformly.

Table 2: Uncertain parameter multipliers assigned uniform distributions

Parameter	Lower Bound	Upper Bound	Description
UQ_gas	0.5	1.0	Fraction of "gaseous" products in the gas phase
UQ_char	0.9	1.1	Char mass fraction of decomposition products
UQ_Vol	0.5	1.0	Porous volume available to the gas
UQ_k	0.65	1.35	Thermal conductivity of foam
UQ_Cp	0.8	1.2	Specific heat of foam

Finally, some parameters are thought to be known with some degree of confidence, and the bounds are also fairly well understood. For these parameters, a triangular distribution is utilized, which has a well-defined mode, as well as bounded extremes. Table 3 includes the two parameters that are modeled with a triangular distribution. In this case, the distributions of both parameters are chosen to be symmetric, though that is not necessary for a generic triangular distribution.

Table 3: Uncertain parameter multipliers assigned triangular distributions

Parameter	Lower Bound	Mode	Upper Bound	Description
UQ_MW	0.65	1	1.35	Molecular weight of org. products
UQ_rho	0.9	1	1.1	Bulk density of foam

The largest complete LHS study varying all nine uncertain parameters consisted of 640 simulations. The parameters were varied in such a way such that smaller, complete LHS studies (20, 40, 80, 160, 320) are subsets of the larger study. Both the temperatures at the experimental thermocouple locations and the can pressures were calculated and recorded as a function of time during the simulations.

2.2. Pressure Distribution

The pressure values at the end of the simulations (1500 sec) are compiled into a histogram which is displayed in Figure 6. The distribution in Figure 6 does not appear to be Gaussian. The pressure distribution exhibits asymmetric behavior. There are a number of possible statistical distributions which can be assigned to the histogram. This report will primarily consider the log-normal distribution.

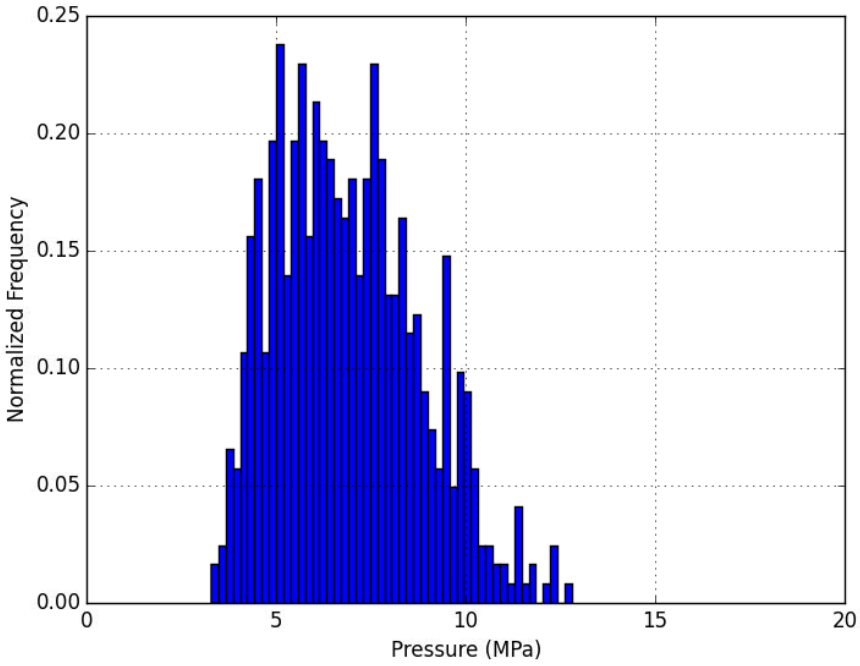

Figure 6: Histogram of final pressure from 640 LHS simulations

The probability distribution function for the log-normal distribution is given as:

$$f(x) = \frac{1}{x\sigma\sqrt{2\pi}} e^{-\frac{(\ln x - \mu)^2}{2\sigma^2}}$$

There is some support for selecting a log-normal distribution other than a qualitative agreement with the shape of the pressure histogram. The log-normal distribution is appropriate for describing the product of random numbers, and the nature of the ideal gas law, combined with the uncertainties of the relevant variables results in a log-normal-like response.

Using a python script to compile all the results, a log-normal distribution curve can be fit to the data, as seen in Figure 7. Since the LHS study is not a comprehensive examination of all parameter combinations, the range indicated by the log-normal distribution is more relevant than the actual minimum and maximum values from the LHS study. Since the log-normal distribution is unbounded, thresholds must be defined to establish useful bounds. The upper bound is set by determining the pressure value for which the CDF is 0.999. This value was selected because it gave a reasonable upper bound based on observation of the log-normal curve and the data:

$$P_{high} = e^{\sqrt{2}\sigma \cdot erf^{-1}[2(0.999-0.5)]+\mu}$$

The lower bound is finite, but based on the observed distributions (e.g. Figure 7), an appropriate lower bound can be defined in a manner similar to that of the upper bound. The lower bound is set by determining the pressure value for which the CDF is 0.001:

$$P_{low} = e^{\sqrt{2}\sigma \cdot erf^{-1}[2(0.001-0.5)]+\mu}$$

The calculated range of the log-normal distribution for pressure at the simulation conclusion (1500 sec) spans 2.8 to 15.4 MPa. The mode is 6.2 MPa.

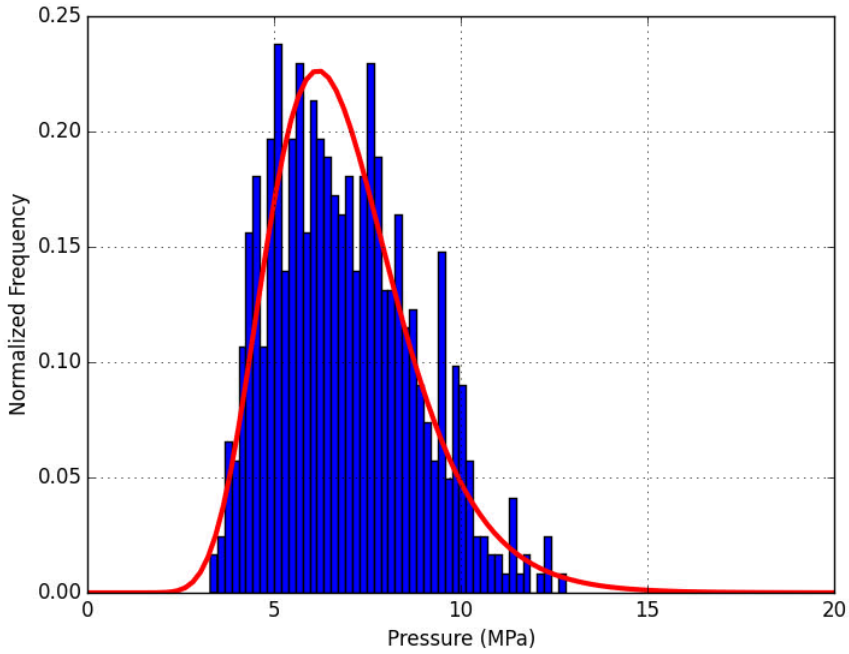

Figure 7: Histogram of final pressure from 640 LHS simulations, with log-normal distribution fit to the data

As discussed in the background section, the uncertainty of simulation pressurization predictions has traditionally been described by a pressure multiplier that is applied to the nominal simulation. If the mode is taken as the nominal response, the equivalent pressure multipliers can be calculated:

$$\lambda_{low} = \frac{2.8\ MPa}{6.2\ MPa} = 0.45$$

$$\lambda_{high} = \frac{15.4\ MPa}{6.2\ MPa} = 2.5$$

These pressure multiplier values are consistent with the values of 0.5 and 2.2 for REF presented in [9] and discussed above. More encouragingly, the pressure multipliers for PMDI have been calculated and used previously (see [5], [13]), and they ranged from 0.5 to 2.6, which are also very close to the values derived here.

2.3. Effect of Number of Runs

The LHS approach can be an efficient way to sample a large parameter space, however care should be taken to ensure a sufficient number of simulations have been completed. The number of uncertain parameters that are being varied often drives the minimum size of the LHS study.

Figure 8 shows the fitted log-normal distributions of the final simulation pressure for various sized LHS studies. Four study sizes, 80, 160, 320 and 640 simulations are all considered; the smaller simulation studies are subsets of the larger studies. It does not appear that the distributions are sensitive to the study sizes shown.

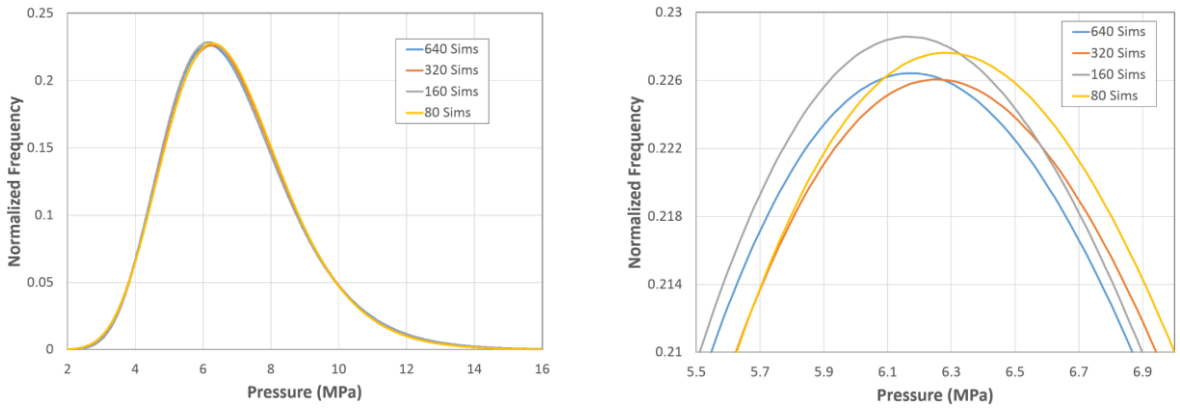

Figure 8: Fitted log-normal distributions for LHS studies of various sizes (80-640 simulations)

In addition to the qualitative comparison in Figure 8, Figure 9 provides a more quantitative comparison of the distribution bounds and mode as a function of LHS study size. For simulation sizes below 80 simulations, the values are subpar, though reasonable, all the way down to 20 simulations. There is some oscillatory behavior (especially of the upper bound) between 80 and 640 simulations; it is unknown whether additional simulations would eventually show convergence to a single value. Regardless, the oscillations occur over a relatively small range of pressures, and the number of simulations (640) is taken to be sufficient.

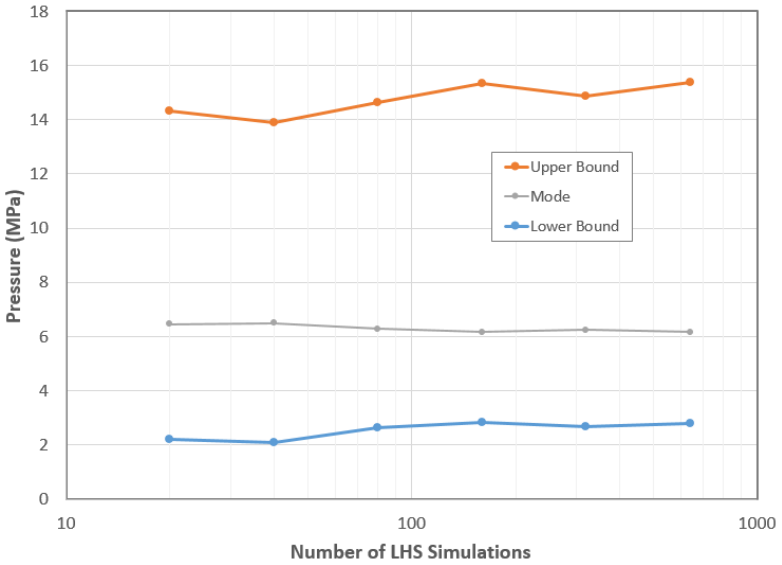

Figure 9: Upper and lower bounds, as well as the mode of the fitted log-normal distribution as a function of the size of the LHS study

2.4. Time Dependency

As discussed in the background section, in previous work, the uncertainty of simulation pressurization predictions has been described by an algebraically-derived pressure multiplier that is applied to the nominal simulation results. This pressure multiplier can be nearly reproduced by taking the bounds from a log-normal distribution fit of the LHS results for pressure at the end of the simulations.

It is also possible to derive a log-normal fit for each time-step of the LHS simulations, and derive the UQ bounds as a function of time. Figure 10 compares the bounds predicted by the pressure multiplier, the bounds associated with the time-dependent log-normal distribution, and the minimum/maximum pressure values from the LHS simulations.

This has the distinct advantage of indicating which times within the simulation are more or less uncertain. For instance, it is known that early in the simulation, before foam begins decomposing, the uncertainty bounds are much smaller than the 0.45 and 2.5 multipliers calculated above. Figure 11 is an early-time view of the curves plotted in Figure 10. It can be seen that the pressure multiplier, which is applied to pressure values for all times, significantly over- and under-predicts the range of pressures from the simulations before the foam has begun decomposing. The bounds defined by the log-normal distribution exhibit occasional excursions due to the sensitivities of the 0.1% bounds when applied to the narrow distribution of pressures at early time.

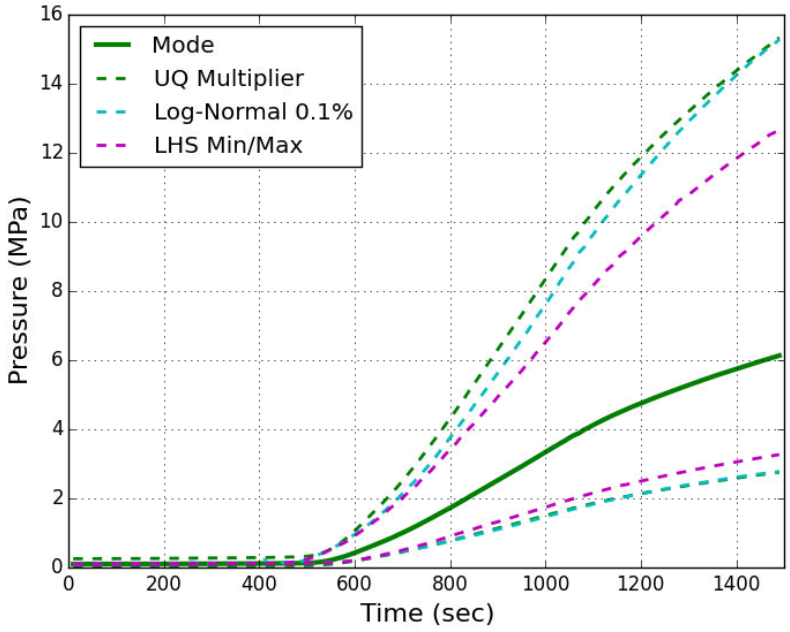

Figure 10: Comparison of UQ bounds defined by the pressure multiplier (green) the time-dependent log-normal distribution (cyan), and the min/max from the LHS simulations (magenta)

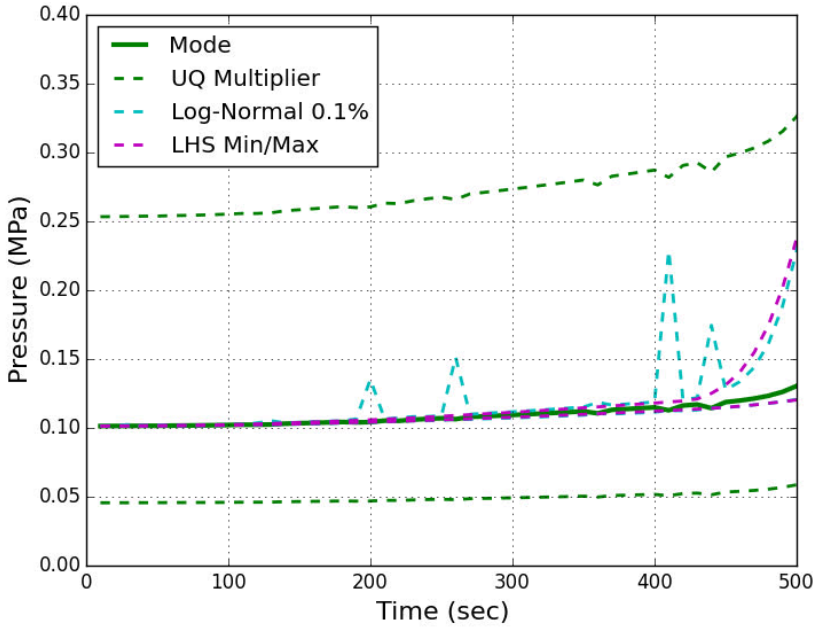

Figure 11: Zoomed in view of data from Figure 10 from 0 to 500 seconds

Figure 12 is a plot of the distribution of pressures at early time before decomposition begins. The distribution appears to be much more symmetric and Gaussian than the distributions in late time (e.g. Figure 7). A consideration should be made in future analyses to use an alternate distribution, or even select a time-dependent distribution that will vary according to the evolving distribution of the pressure. A more flexible approach may also prevent overly-conservative distribution bounds. Figure 13 shows an example of where one of the LHS simulation pressure results exceeds the bounds of the fitted distribution. This phenomenon is limited to relatively low pressure and intermediate times (i.e. 450 seconds in the case of Figure 13), but is an undesirable short-coming of the log-normal distribution fit.

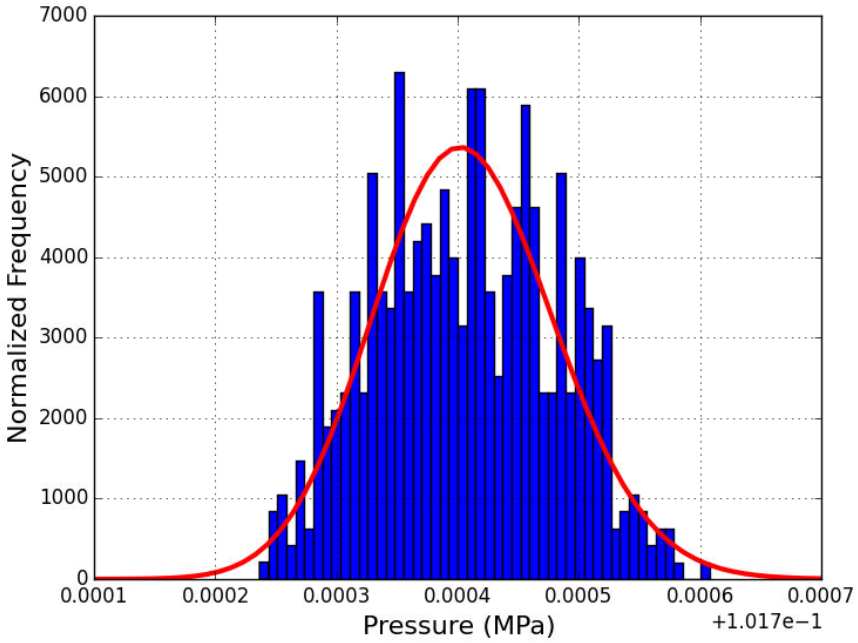

Figure 12: Early time (100 sec) distribution of pressures produced by the LHS study

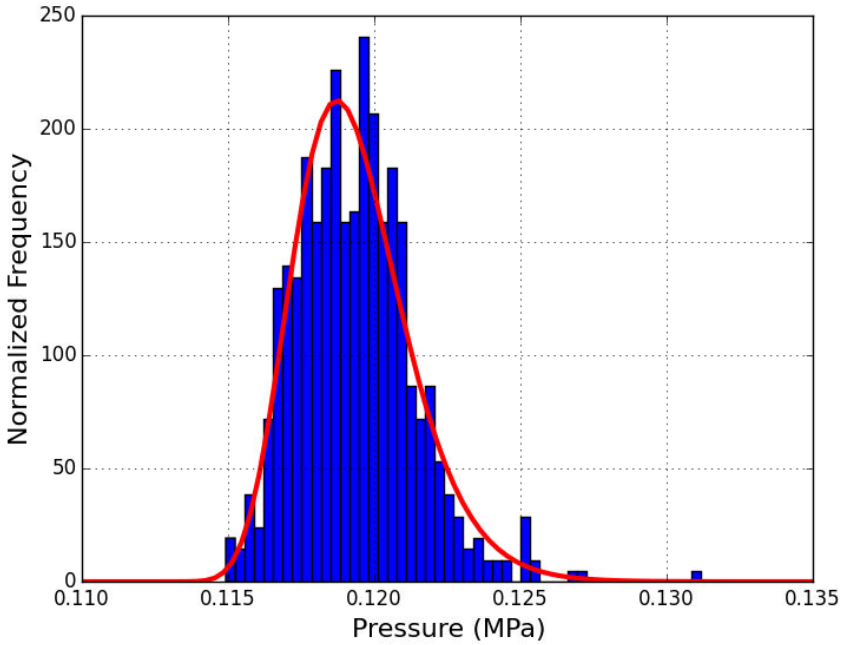

Figure 13: Example of a time (450 sec) when a LHS simulation predicts a pressure outside of the bounds of the log-normal distribution

2.5. Parameter Sensitivity

It is desirable to know which input parameters most strongly influence the simulation response(s) of interest, and in what way. Correlation coefficients can be a powerful tool for examining these relationships. This information can motivate additional model development or guide future experiments. At the conclusion of this LHS study, Pearson correlation coefficients were

calculated. See [9], which contains a description of the Pearson correlation coefficient. Figure 14 shows the correlation coefficients with respect to pressure for all nine parameters as a function of time.

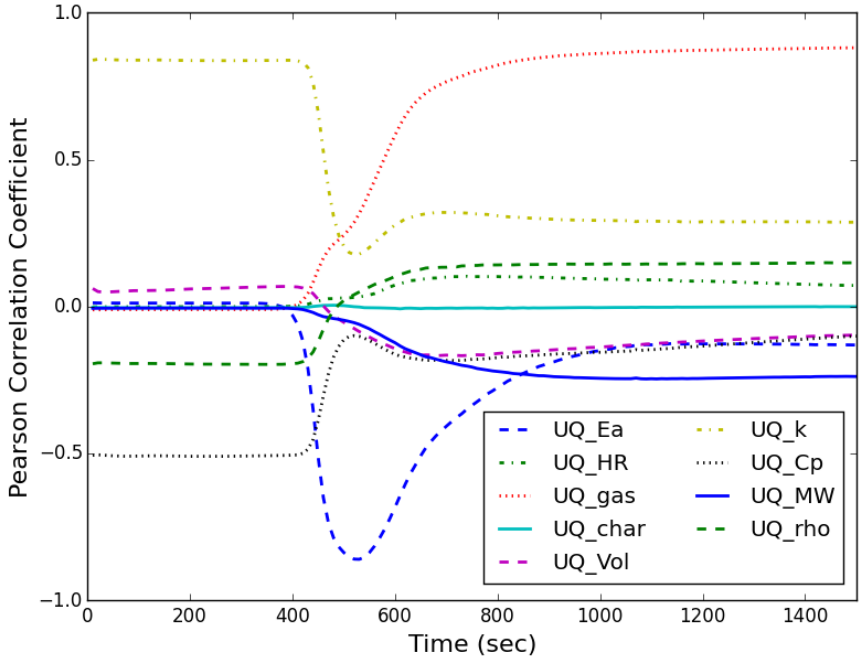

Figure 14: Pearson correlation coefficients of all nine parameters with respect to pressure as a function of time

Note that in early time, Figure 14 shows that all of the most impactful parameters (i.e. UQ_k, UQ_rho, and UQ_Cp) are virgin foam parameters. That is because in early time, decomposition has not yet begun, so it is expected that the decomposition parameters would all have near zero effect. At approximately 400 seconds, the can has heated up sufficiently such that the foam begins to decompose, and the nature of the correlation coefficients changes dramatically. In addition to the virgin foam parameters losing importance, UQ_Ea, corresponding to the reactions' activation energy, begins to rapidly rise, peaking at approximately 500 seconds. This dominance is transient, decaying back down to a lower value once most of the decomposition processes have ended.

Late in time, the three largest influences on pressure are UQ_gas, UQ_k, and UQ_MW. The smallest contributor of these is UQ_MW, which acts as a multiplier on the molecular weight of the organic decomposition gases – this reflects the uncertainty about what the large molecular weight organic gas products are. The relationship to pressure has a negative correlation, since a larger molecular weight corresponds to fewer moles of gas for a given mass. Some of the uncertainty can be reduced by additional experimental measurement, but some may not be resolved so easily. There may be a model form error if a portion of the decomposition products are pressure or temperature dependent (i.e. the model may be missing additional chemistry). Regardless, much of the decomposition gas (approximately 33% by mass) is made up of CO_2; the fraction by moles of gas is even greater due to the lower molecular weight of CO_2 relative to the other high molecular weight products. Of course, there is no uncertainty with respect to the molecular weight of CO_2. Thus, the UQ_MW parameter is only describing the uncertainty of the fraction of the gas

corresponding to the higher molecular weight products. This is why it does have a higher magnitude correlation with pressure.

The second largest correlation coefficient is a positive one with respect to UQ_k. That is, larger foam conductivity values correspond to larger pressure predictions. The more efficient transfer of heat throughout the domain must be increasing the pressure either by increasing the gas temperature, or by spurring on the decomposition of more foam, leading to more moles of gas (or a combination of both).

The most influential parameter, however, dwarfs the other eight parameters. UQ_gas corresponds to the fraction of "gaseous" products that are actually in the gas phase (as opposed to the liquid phase). This is manifested in the simulation by distributing the original mass fraction of the organic products into the gas and solid char phases. It is assumed that the high molecular weight organic gases have a relatively low vapor pressure and may condense to a liquid, resulting in a lower gas pressure. Thus, a large positive correlation is observed, since large values of UQ_gas correspond to most of the decomposition products remaining uncondensed in the gas phase. This analysis is helpful as a signpost to indicate the direction of research that will most help resolve uncertainty about the pressure. Specifically, the lack of knowledge about the phase of the decomposition products is a significant source of uncertainty, therefore, developing a vapor-liquid equilibrium model should be a priority.

2.6. Comparison to Experiment

Figure 15 displays the mode as well as the UQ bounds associated with the computed log-normal distribution bounds previously detailed in Figure 10. Also plotted are two instances of the experimental data from Figure 4, one for each the upright and inverted configurations. As can be seen, the uncertainty bounds completely bracket the experimental data.

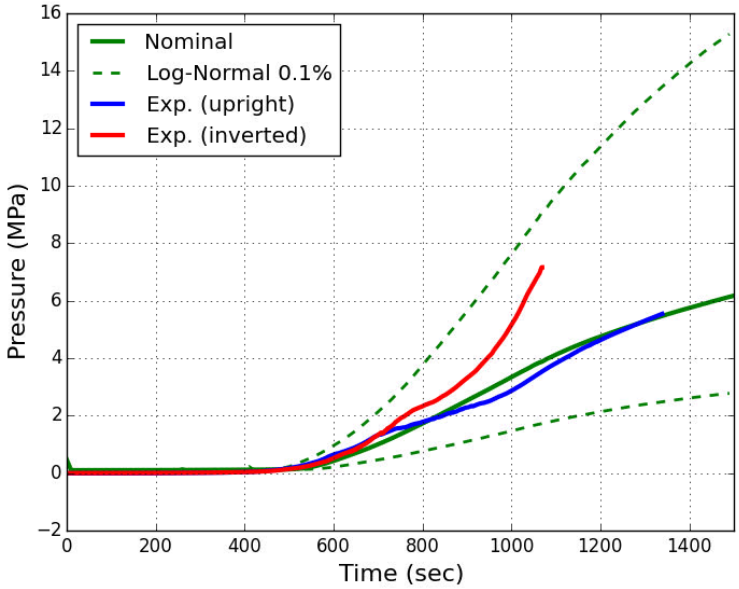

Figure 15: Comparison of upright and inverted experiments to simulation with calculated uncertainty

As discussed above, when comparing the pressure multipliers to previous work, these bounds are consistent with the previous PMDI model validation study [5].

3. DISCUSSION

The main goal of this report is to bring the uncertainty associated with pressure due to foam decomposition into a framework similar to the rest of the uncertainty quantification analyses with regards to thermal modeling. However, it should be regarded as part of the progression of uncertainty quantification of pressurization, as opposed to the conclusion. There are still outstanding questions about the definitions of the uncertainty parameters (i.e. triangular, normal, uniform) and their ranges. Furthermore, the assumed log-normal distribution of the pressure may not be appropriate for all times, and it may be made to be more adaptable using advanced UQ methodologies.

There are additional model parameters that have been omitted from this analysis which may be appropriate to include in future studies. For instance, the uncertainty in the progression of the foam decomposition reactions has been distilled to a single activation energy multiplier and the mass fraction of the residual char. This is believed to bracket all of the uncertainty associated with the decomposition model derived from experimental TGA data; in fact, this study has shown that the mass fraction of char plays almost no role in the evolution of the foam-in-can simulation (see Figure 14). However, the assumption has not been rigorously examined, and there are other decomposition model parameters that remain uninvestigated, including reaction-specific activation energies, pre-exponential factors, mass-fractions, and the order of the reactions. These parameters do not address the possibility that the assumption of the decomposition process consisting of pressure-independent, uncoupled Arrhenius reactions is incorrect.

Several of the uncertainties detailed in the LHS study correspond to what can be regarded as model form errors. That is, even if most of the model parameters are known perfectly, a finite uncertainty must still be applied to account for physics that are being neglected. In this case, both the fraction of "gaseous" products in the gas phase and the porous volume available to the gas both represent parameters that cannot be refined without additional models. A vapor-liquid equilibrium model may reduce the uncertainty in the quality of the decomposition products. A model that predicts pore wall failure as a function of pressure and temperature may help to reduce the uncertainty of the porous volume available to the gas.

However, supposing these models were instituted, the narrowing of the uncertainty bounds may be misleading. There is spread in the experimental data between upright and inverted experiments due to the presence of gravity and its associated effects. Gas and liquid transport are likely important physics that are gravity-dependent, but not included in the current model. It does not follow that the absence of model parameters associated with missing physics results in less uncertainty with regards to predicting experimental data. Only the uncertainty of the simplified model itself, constrained by its (possibly problematic) assumptions, is low. Physical insights from the analyst, both from knowledge of the problem being solved and careful evaluation of the experimental data, are still necessary to improve model predictiveness and accurately represent uncertainty.

4. REFERENCES

[1] *Sierra Thermal/Fluids Code,* Albuquerque, NM: Sandia National Laboratories, 2012.

[2] S. Scott, A. Dodd, M. Larsen and J. Suo-Anttila, "Validation of Heat Transfer, Thermal Decomposition, and Container Pressurization of Polyurethane Foam using Mean Value and Latin Hypercube Sampling Approaches," *Fire Technology,* 2014.

[3] L. Phinney, C. Safta, L. Hund, V. Brunini, R. Garcia, R. Keedy and P. Hough, "PMDI Polyurethane Foam Thermal Conductivity, SAND2016-1888," Sandia National Laboratories, Albuquerque, NM, 2016.

[4] P. Hough and J. Templeton, "Addendum to Quantification of Margins and Uncertainties for the W87 Thermal Race in a Directional Abnormal Thermal Environment, SAND2015-4564," Sandia National Laboratories, Alburqueque, NM, 2015.

[5] S. Scott, A. Dodd, M. Larsen, J. Suo-Anttila and K. Erickson, "Validation of Heat Transfer, Thermal Decomposition, and Container Pressurization of Polyurethane Foam, SAND2014-17867," Sandia National Laboratories, Albuquerque, NM, 2014.

[6] A. Saltelli, K. Chan and E. M. Scott, Sensitivity Analysis, New York: John Wiley and Sons, Inc., 2000.

[7] J. C. Helton and F. J. Davis, "Latin Hypercube Sampling and the Propagation of Uncertainty in Analyses of Complex Systems," Sandia National Laboratories, Albuquerque, NM, 2001.

[8] B. Adams, L. Bauman, W. Bohnhoff, K. Dalbey, M. Ebeida, J. Eddy, M. Eldred, P. Hough, K. Hu, J. Jakeman, L. Swiler and D. Vigil, "DAKOTA, A Multilevel Parallel Object-Oriented Framework for Design Optimization, Parameter Estimation, Uncertainty Quantification, and Sensitivity Analysis: Version 5.4 User's Manual," Sandia National Laboratories, Albuquerque, NM, 2013.

[9] R. Keedy, A. Hetzler and A. Dodd, "Validation and Uncertainty Quantification of Removable Epoxy Foam (REF) Thermal Decomposition and Pressurization Model," Sandia National Laboratories, Livermore, CA, 2015.

[10] J. Suo-Anttila, J. Koeing, A. Dodd, C. Robino and E. Quintana, "Thermal-Mechanical Exclusion Region Barrier Breach Foam Experiments (L2 Milestone in FY13), SAND2013-7346," Sandia National Laboratories, Albuquerque, NM, 2013.

[11] S. N. Scott, M. E. Larsen, A. B. Dodd and K. L. Erickson, "Model validation of thermal decomposition and container pressurization of polyurethane foam," in *Interflam*, Windsor, UK, 2013.

[12] R. Keedy and A. Dodd, "Thermal Conductivity Models of PMDI and TDI Foams in Abnormal Thermal Environments," Sandia National Laboratories, Livemore, CA, 2015.

[13] K. Erickson, A. Dodd, R. Hogan and K. Dowding, "Heat Transfer, Foam Decomposition, and Container Pressurization: Comparison of Experimental and Modeling Results," in *Proceedings of Interflam*, 2010.

DISTRIBUTION

1	MS0447	Katie Goodner	10631
1	MS0825	Roy Hogan	1514
1	MS0828	James Yuan Hartley	1514
1	MS0828	Adam Hetzler	1544
1	MS0828	Tito Silva	1514
1	MS0828	Walt Witkowski	1544
1	MS0836	Dean Dobranich	1514
1	MS0836	Tre Shelton	1514
1	MS0840	Tim Koehler	1513
1	MS1135	Jill Suo-Anttila	1532
1	MS9159	Patty Hough	8954
1	MS9159	Cosmin Safta	8954
1	MS9403	Joe Cordaro	8344
1	MS9957	Myra Blaylock	8253
1	MS9957	Victor Brunini	8253
1	MS9957	Amanda Dodd	1914
1	MS9957	Tricia Gharagozloo	8253
1	MS9957	Erin Mussoni	8253
1	MS9957	Sarah Scott	8253
1	MS9957	Jeremy Templeton	8253
1	MS0899	Technical Library	9536 (electronic copy)


Sandia National Laboratories